Molecular Vision 2019; 25:745-755 <http://www.molvis.org/molvis/v25/745>
Received 23 May 2019 | Accepted 11 November 2019 | Published 14 November 2019

Arresting proliferation improves the cell identity of corneal endothelial cells in the New Zealand rabbit

Carlos-Alberto Rodríguez-Barrientos,[1,2] Victor Trevino,[1] Judith Zavala,[1] María-Dolores Montalvo-Parra,[1] Guillermo-Isaac Guerrero-Ramírez,[1] Raul Aguirre-Gamboa,[1] Jorge-Eugenio Valdez-García[1]

[1]Tecnologico de Monterrey, Escuela de Medicina, 3000 Morones Prieto Ave., Col. Los Doctores, Monterrey, N.L., Mexico; [2]Universidad de Oviedo, Instituto Universitario Fernández-Vega, Asturias, Spain

Purpose: Corneal endothelium engineering aims to reduce the tissue shortage for corneal grafts. We investigated the impact of mitogenic and resting culture systems on the identity of corneal endothelial cells (CECs) for tissue engineering purposes.

Methods: Rabbit CECs were cultured in growth factor-supplemented media (MitoM) until confluence. At the first passage, the CECs were divided into two populations: P1 remained cultured in MitoM, and P2 was cultured in a basal medium (RestM) for another passage. Morphologic changes in the CECs were analyzed, and RNA was isolated for transcriptome analysis. Quantitative PCR and immunocytochemistry validation of selected differentially expressed markers were performed.

Results: The CECs in MitoM showed fibroblastic morphology, whereas the CECs in RestM exhibited polygonal morphology. Circularity analysis showed similar values in human (0.75±0.056), rabbit basal (before cultured; 0.77±0.063), and CECs in RestM (0.73±0.09), while MitoM showed lower circularities (0.41±0.19). Genes related to collagen type IV and the extracellular matrix, along with the adult CEC markers ATP1A1, ATP1B1, COL8A2, GPC4, and TJP1, were highly expressed in RestM. Conversely, the *IL-6, F3,* and *ITGB3* genes and the non-adult CEC markers *CD44*, *CNTN3*, and *CD166* were more expressed in MitoM. Overall, from the transcriptome, we identified 832 differentially expressed probes. A functional analysis of the 308 human annotated differentially expressed genes revealed around 13 functional clusters related to important biological terms, such as extracellular matrix, collagen type 4, immune responses, cell proliferation, and wound healing. Quantitative PCR and immunocytochemistry confirmed the overexpression of ATP1A1, TJP1, and GPC4 in CECs in RestM.

Conclusions: The addition of a stabilization step during CEC culture improves the cells' morphology and molecular identity, which agrees with transcriptome data. This suggests that stabilization is useful for studying the plasticity of the corneal endothelium's morphology, and stabilization is proposed as a necessary step in corneal endothelium engineering.

Corneal diseases represent the second leading cause of blindness, affecting 4.9 million people worldwide; these individuals could potentially have their sight restored through corneal transplantation [1,2]. Penetrating keratoplasty is the standard procedure used for the treatment of corneal blindness. However, this procedure faces two primary problems: a shortage of graft donors and a decrease in endothelial cell density within 5 years of transplantation [3].

The corneal endothelium (CE) is responsible for maintaining corneal hydration through a pump–leak mechanism [4]. Although CE cells (CECs) are normally arrested in the early G1 phase of the cell cycle, they retain their proliferative capacity [5]. Tissue engineering can take advantage of this capacity to address the lack of available donor tissue. To accomplish this aim, a robust system for the isolation and propagation of CECs is needed. Several studies exploring complex culture media have reported the increased proliferative capacity of CECs [6-10]. The addition of growth factors to culture media enhances CEC proliferation; however, this effect is associated with changes in cell morphology (from hexagonal to fibroblastic) and alterations in the expression of characteristic molecular markers, which raises questions concerning the CECs' identity [6,8,11-13]. The use of culture media without growth factors is able to maintain the hexagonal morphology of the CECs; however, it yields low proliferation rates that cannot be propagated beyond the first passage [10,14].

In this study, with the aim of improving the identity of CECs after proliferation, we first used a widely used supplemented culture medium to proliferate CECs [9], which was then followed by a resting step that incorporated basal medium to provide evidence of the development of a convenient CEC expansion strategy. We compared the morphology and transcriptome of CECs in two conditions and validated CEC markers using immunohistochemistry and

Correspondence to: Victor Trevino, Tecnologico de Monterrey, Escuela de Medicina, Morones Prieto Ave. 3000, Col. Los Doctores, Monterrey, N.L., Mexico, 64710; Phone: +52 81 88882045; email: vtrevino@tec.mx

quantitative PCR. The results suggest that the resting step helps maintain the identity of cultured CECs.

METHODS

This study was approved by the institutional local ethics committee (School of Medicine of Tecnologico de Monterrey), number 2013-Re-002. All animals were treated according to the Guide for the Care and Use of Laboratory Animals adhering to the guidelines for the human treatment and ethical use of animals for vision research stated by the Association for Research in Vision and Ophthalmology.

Corneal endothelial tissue isolation: Eight corneas were obtained from four 3-month-old New Zealand rabbits weighing about 3 kg. The rabbits were euthanized under general anesthesia with 30 mg/kg of ketamine (Pisa Farmaceutica, Guadalajara, México), followed by a lethal intracardiac injection of sodic pentobarbital (Pets Pharma, Estado de Mexico, Mexico). The corneas were excised, rinsed with OptiMEM-I (Gibco®; Thermo Fisher Scientific, Waltham, MA) supplemented with 8% fetal bovine serum (FBS; Cellgro, Manassas, VA) and 1% streptomycin/penicillin antibiotics (Thermo Fisher Scientific), and placed in a sterile tissue culture dish. Two sets of rabbits were used at different times. The first set of two rabbits was used for culture followed by transcriptome analyses while the second was used for culture followed by validation (immunocytochemistry and quantitative PCR [qPCR]).

Isolation of CECs: CECs were isolated using the "peel-and-digest" approach. Briefly, using sterile surgical forceps, Descemet's membrane (DM) with the intact endothelium (DM/CE) was carefully dissected from the corneal stroma, and then was washed several times with Dulbecco's Modified Eagle Medium: Nutrient Mixture F-12 (DMEM-F12, Gibco®; Thermo Fisher Scientific, Grand Island, NY) supplemented with 10% FBS and 1% antibiotic combination. DM/CE complexes were incubated in OptiMEM-I 8% FBS and the 1% antibiotic combination overnight to stabilize the cells before culture. They were then incubated with 2 mg/ml of collagenase type I (Sigma-Aldrich Co., St. Louis, MO) at 37 °C for 1 h to release the CECs from DM. CEC clusters were treated with trypsin/EDTA (0.25% trypsin/0.53 mM EDTA; Sigma-Aldrich Co.) for 10 min to dissociate aggregates into smaller cell clumps. They were collected following centrifugation at 375 ×g for 10 min.

CEC culture: CECs were first cultured in a previously reported medium (MitoM) [9] containing OptiMEM-I supplemented with 8% FBS, 20 ng/ml of nerve growth factor (NGF; Sigma-Aldrich Co.), 5 ng/ml of epidermal growth factor (EGF; Sigma-Aldrich Co.), 100 µg/ml of pituitary extract (Sigma-Aldrich Co.), 200 µg/l of calcium chloride (Sigma-Aldrich Co.), 20 µg/ml of ascorbic acid (Sigma-Aldrich Co.), 0.08% chondroitin sulfate (Sigma-Aldrich Co.), and antibiotics. Isolated cells were incubated at 37 °C in a 5% CO_2 humidified atmosphere. The medium was changed every third day until 80% confluence. At passage 1, the CECs were subcultured at a 1:2 split ratio. Population 1 continued to be cultured in MitoM, while population 2 was cultured in OptiMEM-I supplemented with only 8% FBS and 1% antibiotics (RestM) up to 80% confluence for an additional passage. We refer to the RestM procedure as "resting" because it lacks growth factors to decrease proliferation rates. An Axiovert 40 CFL contrast microscope (CFL; Carl Zeiss AG, Oberkochen, Germany) featuring a PowerShot A640 digital camera (Canon Inc., Tokyo, Japan) was used to register cell morphology.

Morphology analysis: NIH Image J software [15] was used to analyze the morphology of human CECs from three healthy biomicroscopies from a public database [16], basal rabbit CECs (before culture), in MitoM and RestM. A similar scale was set on each photograph. Then about 40 CECs were delimited and analyzed for human MitoM and RestM, whereas about 20 cells were analyzed for basal rabbit CECs with free shape region of interest. Area and perimeter were obtained using Image J (Analysis menu, Measure tool). Circularity was calculated as 4π (area/perimeter^2), and values near from 1 were taken as high circularity indices, thus near hexagonality [17].

Cellular yield analysis: Cellular yield was calculated for CECs cultured in MitoM and RestM. For this analysis, the quotient of cellular concentration (cells/ml) at the end of passage 2 divided by the cellular concentration at the end of passage 1 was calculated for each culture condition (MitoM and RestM). The average and the standard error were calculated. A *t* test was used to analyze statistically significant differences between the calculated yields.

RNA isolation: Total RNA was extracted with the RNeasy mini Kit (Qiagen, Hilden, Germany) from CECs before culture, and then after culture in MitoM and RestM. Cells were harvested at 80–90% confluence around day 9 of culture. RNA concentration and purity were determined by spectrophotometry using a NanoDrop ND-1000 UV-VIS spectrophotometer (Waltham, MA); only RNA samples with an A260/A280 ratio ≥1.8 were used for further experiments. The Experion RNA HighSense (Hercules, CA) was used to determine the concentration and integrity of mRNA. Yields were 62–182 ng/µl per confluent dish, and a total of 3 µg/µl was used for sample preparation.

Microarray hybridization: RNA preparation, labeling, and hybridization were performed according to the manufacturer's recommendations (Agilent Technologies, Santa Clara, CA) using the customized rabbit microarray (G2519F) containing around 44,000 probes. Briefly, cyanine-3- (Cy3-) and cyanine-5 (Cy5)-labeled cRNA were prepared from the total RNA using a labeling kit (Quick Amp; Agilent Technologies). This was followed by column purification (RNeasy Mini Kit; Qiagen). Cy3 was used for the CECs in MitoM, and Cy5 was used for the CECs in RestM. Dye incorporation and cRNA yield were assessed with spectrophotometry (ND-1000; Thermo Fisher Scientific). Equal amounts of the Cy3- or Cy5-labeled cRNA mixture were hybridized to the microarrays (Rabbit Gene Expression Microarrays; Agilent) for 17 h at 65 °C in a rotating hybridization oven (Agilent), followed by washing and scanning. Data were obtained immediately after washing on a microarray scanner (GenePix 4000B; Molecular Devices LLC, Sunnyvale, CA).

Microarray data analysis: The R statistical environment was used to process and analyze the data (https://cran.r-project.org/). Raw data were transformed using $\log_2$ and subsequently, were quantile-normalized before statistical analysis. The differentially expressed genes were obtained with a paired *t* test that was conducted between the four replicates of MitoM and RestM. A functional analysis of the differentially expressed genes was performed using the Database for Annotation, Visualization, and Integrated Discovery (DAVID) [18]. Only those probes with human annotations were used for this process. Each microarray probe was aligned to the human transcriptome annotations (hg19) using BLAST (included in Appendix 1). Only those DAVID terms where the p value was less than 0.01, the adjusted false discovery rate p value was less than 0.25, and the gene count was greater than three were examined.

Quantitative PCR: Validation of expression levels for different corneal endothelial markers was performed by quantitative PCR (qPCR) using (m)RNA from CECs before culture, after cultured in MitoM, and RestM. Primers design was conducted in Blast Primer platform (NCBI) and synthetized by T4 oligo company (Guanajuato, Mexico). GAPDH F: CGA GCT GAA CGG GAA ACT CA, R: CCC AGC ATC GAA GGT AGA GG; ATP1A1 F:GAT CCA CGA AGC TGA CAC GA, R: CTG TTA CAG AGG CCT GCG AT; GPC4 F: CGC CAA ATC ATG GCT CTT CG, R: GGC ACT GCT GGT ACT CAC AT; BTG2 F: GGC TTA AGG TTT TCA GCG GG, R: CTT GTG GTT GAT GCG GAT GC; TJP1 F: CTC AAG TTC CTG AAG CCC GT, R: TAG GAT CAC CCG ACG AGG AG. Amplification was performed with the PowerUp SYBR Green Master Mix kit in a Step One 48-well thermocycler (Applied Biosystems, Foster City, CA), under these conditions: initial denaturing at 95 ºC 1 min, 40 cycles: 95 ºC/30 s, 61 ºC/30 s, 72 ºC/30 s; final extension 72 ºC/5 min. Finally, ΔCt method was used to analyze expression levels.

Immunocytochemistry: Immunocytochemistry was performed in CECs before culture, after culture in MitoM, and in RestM to analyze the presence of GPC4 (Abcam, ab150517, Cambridge, UK), CD166 (Abcam, ab78649), ZO-1/TJP1 (ThermoFisher, 61–7300, Waltham, MA), and Na/K-ATPase (Abcam, ab176163, Cambridge, UK). Immunocytochemistry consisted of overnight cell stabilization over coverslips with poly-D lysine (Sigma-Aldrich, P7280), fixation with 4% paraformaldehyde, nonspecific bonding blockage with 5% bovine serum albumin (BSA; Sigma-Aldrich, A-7030), overnight 4 °C incubation with primary antibodies (GPC4 5 µg/ml, CD166 1 µg/ml, ZO-1 5 µg/ml, and Na/K-ATPase 1:100), and incubation with Alexa Fluor 488 secondary antibody (Abcam, ab150077) for 1 h at room temperature. Fluoroshield Mounting Medium with 4′,6-Diamidine-2′-phenylindole dihydrochloride (DAPI; Abcam, ab104139) counterstain was used. For the complete corneas, we followed a previously described protocol for immunostaining on a flat-mounted whole intact cornea [19]. Briefly, corneas were rinsed in Phosphate-Buffered Saline (PBS 1X; 140 mM NaCl, 3 mM KCl, 10 mM $NaPO_4$, pH 7.4 at 25 °C), cut into four pie-shaped wedges and immediately fixed. Fixation occurred for 30 min in 0.5% paraformaldehyde (Sigma-Aldrich Co.) in PBS pH 7.45 at 4 °C. Then, cell membranes were permeabilized with 1% Triton X-100 (Sigma-Aldrich Co.) in PBS for 5 min at room temperature. Blockage of non-specific binding sites was performed by incubation for 30 min at 37 °C with 5% BSA (Sigma-Aldrich Co). Primary and secondary antibodies, as well as counterstaining, were used in the same fashion as for CECs immunocytochemistry but, corneal pieces were fully immersed in the corresponding solutions. Epifluorescence was registered with a widefield fluorescence microscope (Zeiss Imager Z1) with an AxioCam HRm (Zeiss) camera (Göttingen, Germany).

RESULTS

Isolation of corneal endothelial tissue: The peel-and-digest approach for the isolation of CECs yielded small groups of cells that showed a polygonal morphology, and they were cultured in MitoM (Appendix 1). This evidence also support that the protocol was successfully implemented, and that CECs can be used for further experiments.

Effects of culture conditions on the morphology of CECs: The cultured CECs showed variations in morphology throughout the 5 days in MitoM at P0 (Figure 1A–E). The morphological

changes in the CECs in MitoM and RestM culture medium started at around day 2 and became more evident after 5 days of incubation (Figure1B,C). The passaged cells cultured in MitoM acquired a fibroblastic morphology, whereas those in RestM were far less elongated and had formed a monolayer. At day 9, the effect of the MitoM became more evident, particularly when the CECs were compared to those at P0 (Figure 1D). Conversely, the RestM CECs became polygonal (Figure 1C,E). The average of the circularity index of the specular microscopy of the human CECs was 0.79±0.072, of the rabbit CECs before culture was 0.77±0.063, after culture in MitoM was 0.41±0.19, in RestM passage 1 was 0.73±0.09, and in RestM passage 2 was 0.6±0.18 (Figure 1G). There was no statistically significant difference between the circularity of human and basal rabbit CECs or between CECs in RestM P1 and human CECs. The difference in the circularity of human versus MitoM, human versus RestM P2, and basal versus RestM P2 CECs was statistically significant ($p<0.05$). These results showed that the resting phase of this culture system enhances the morphology of the CECs, as they take on a corneal–endothelial-like shape. Nevertheless, these results also warn that prolonged passages may also be detrimental.

Cellular yield analysis: CECs in MitoM showed a fold-change increase in the cellular yield of 1.52 from passage 1 to passage 2, whereas CECs in RestM showed an increase of 1.27 (Figure 2H). Although the difference between the yields obtained in the two culture conditions was not statistically significant ($p=0.2583$), lower proliferation was apparent in RestM.

Gene expression and functional analysis: We first tested whether the cell identities were lost during culture by comparing the overall similarity of normalized gene expressions. Hierarchical clustering showed that those cells in the culture were more similar to those of the subject from which the cells were obtained than to the cells in the culture conditions (Figure 2). Nevertheless, a principal component analysis (PCA) revealed that the major source of variation was the culture condition (Figure 2B), which was confirmed with hierarchical clustering, estimated from 5% of the gene expression profiles that had a higher coefficient of variation (Figure 2C). These results support the validity of the assays, treatments, and collected data.

We then compared the expression of specific CEC markers between the RestM and MitoM conditions. We assessed 26 selected genes (in gene: probeID from Appendix 1 these are *AQP1*: A_04_P030932, *COL8A1*: A_04_P001586, *ATP1A1*: A_04_P004696, *ATP1B1:* A_04_P002527, *TJP1*: A_04_P086632, *TJP2*: A_04_P067042, *CDH2*: A_04_P031967, *SLC4A11*: A_04_P094717, *GPC4*: A_04_P095302, *CD200*: A_04_P095118, *CLRN1*: A_04_P082648, *GLP1R*: A_04_P079252, *CNTN3*: A_04_P098144, *PCDHB7*, *HTRD1*: A_04_P004265, *GRIP1*: A_04_P098464, *PKD1*: A_04_P012501, *ZP4*: A_04_P003166, *CNTN6*: CNTN6, *SLC3A2*: A_04_P003146, *ALCAM/CD166*: A_04_P020128, ERBB2/CD340: A_04_P049357, *CD9*: A_04_P018111, *CD44*: A_04_P101042, *ITGA5/CD49e*: A_04_P088227, and *NT5E/CD73*: A_04_P084588).which serve as markers for adult CECs, fetal CECs, non-fibroblast CEC phenotypes, and fibroblast CEC phenotypes [20,21]. Of these genes, nine demonstrated expression changes ($p<0.05$; Figure 3A).

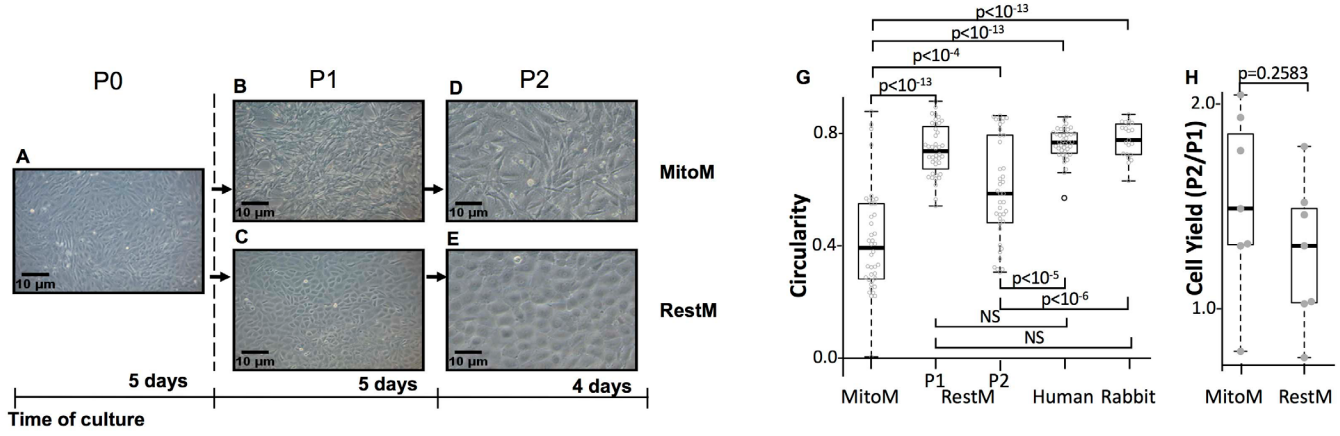

Figure 1. CECs in MitoM and RestM culture conditions. **A**: Corneal endothelial cells (CECs) in MitoM culture conditions at P0 before the subculture (10X). **B**: CECs in MitoM at P1 (10X); and (**C**) CECs in RestM at P1 (10X). **D**: CECs in MitoM at P2 (10X); and (E) CECs in RestM at P2 (20X). **G**: Cellular circularity of human, rabbit basal, MitoM, RestM passage 1 (RestM P1), and RestM passage 2 (RestM P2) CECs. **H**: Cellular yield analysis of CECs obtained after the first passage in MitoM and RestM.

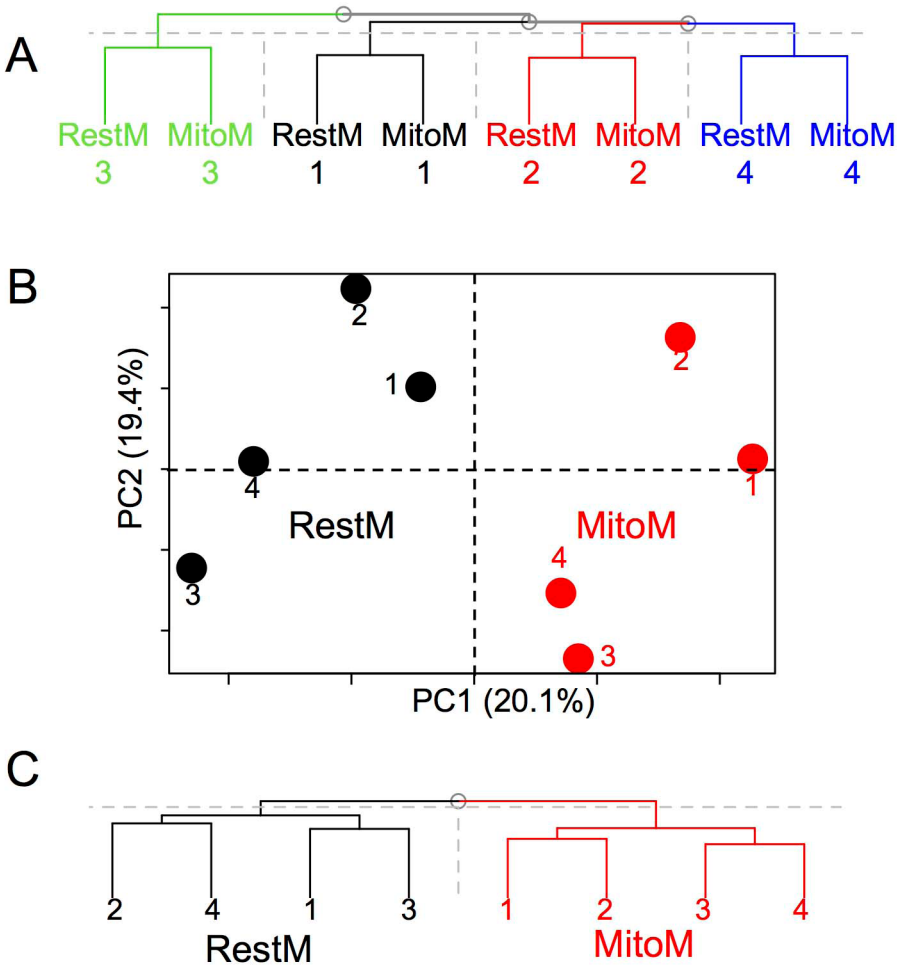

Figure 2. Overall gene expression comparison among the biological replicates 1, 2, 3, and 4. **A**: Hierarchical clustering comparing all probes in the microarray. **B**: First and second principal components. The percentage of the total explained variability is shown in the axis labels. PC1 seems to be associated with treatment. **C**: Hierarchical clustering using 5% of the probes with the highest variability.

The results suggested that adult CECs markers (*ATP1A1, ATP1B1, COL8A2, GPC4, CDH2*, and *TJP1*) were more expressed in the RestM condition, while three non-adult CEC markers (*CD44, CNTN3,* and *CD166*) were more expressed in the MitoM condition. These results showed that markers of specific corneal functions had begun to diverge between the two conditions. Nevertheless, the number of altered genes observed from these CEC markers was too low to compare the overall changes in the biological function. Therefore, to expand the functional analysis, we used the detected differential gene expression profiles to characterize the functional differences in the CECs between the MitoM and RestM conditions. We identified 781 differentially expressed probe genes, as obtained with paired *t* tests between the four replicates of MitoM and RestM at a statistical significance level of $p<0.01$, whose fold change was greater than 1, and had an associated known human gene (Appendix 1).

A DAVID analysis was performed using the 308 unique genes represented in the 781 differential probes. To summarize these results, we performed hierarchical clustering that resulted from the estimated fold change, and which included the intersection of functional terms and genes. From the results shown in Figure 3B, we identified around 13 functional clusters related to extracellular matrix, collagen type 4, protein modifications, response to a stimulus, apoptosis and antiapoptosis, nuclear lumen, ribosome biogenesis, signal transduction, immune responses, cell proliferation, and wound healing, among others. The details of the biological terms are shown in Appendix 2.

From the functional analysis, we chose some functional terms related to relevant biological functions and compared the gene expression levels of the significant genes as the levels related to those functions (Figure 3C). The analysis revealed that CECs in RestM clearly showed a greater expression of genes related to collagen type IV and the extracellular matrix,

suggesting remodeling processes. For example, four types of collagen type IV were overexpressed in RestM together with *TIMP3* to inhibit collagenases. Moreover, they were also overexpressed with *LUM*, which binds collagen fibrils; *SMOC2*, which promotes matrix assembly; and *CRTAP*, which is involved in the hydroxylation of fibrillar collagen. Conversely, in MitoM, *MMP1* was more greatly expressed and it is involved in the cleavage of various types of collagen. The function and expression of these genes suggest that they are associated with the different shapes observed under the microscope.

Although the term cell proliferation showed that similar numbers of genes were more greatly expressed in MitoM and RestM, some of the terms were clearly related to proliferation states, such as nuclear lumen and ribosome biogenesis, which demonstrated higher expression levels in those genes in the MitoM condition. These results suggested that cells in the MitoM condition are more likely to be related to proliferative processes.

In terms of wound healing, CECs in the MitoM condition overexpressed *IL-6*, *F3*, and *ITGB3*, which are related to inflammation, complement cascade, and cell adhesion,

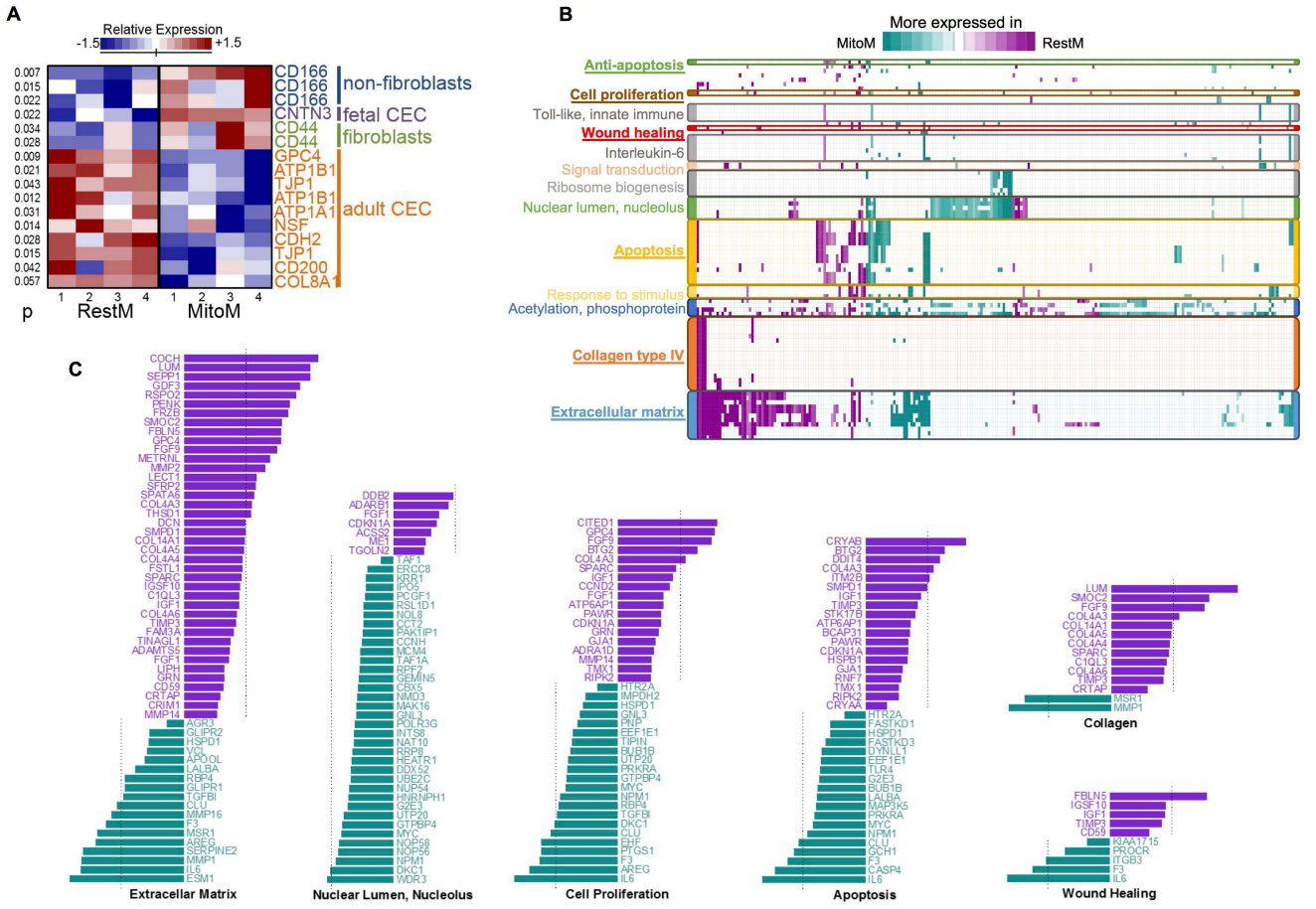

Figure 3. Gene expression comparison and functional analysis. **A**: Differential expressed corneal endothelial cell (CEC) markers between cells cultured in RestM and MitoM. The molecular markers are grouped by type. Only markers close to p=0.05 are shown. Relative expression is estimated in the Z-score (standard deviations from the mean). **B**: Functional analysis of differentially expressed genes. The heat map shows the genes (horizontal axis) contained within functional biological terms (vertical axis). The color represents the fold change in gene expression (cyan is used to represent those genes that were more greatly expressed in MitoM, while purple represents those genes more greatly expressed in RestM). Genes whose *t* test p values were less than 0.01, and which demonstrated a fold change greater than 1, were used. Only over-represented biological terms with a p value of less than 0.01, a false discovery rate of less than 0.25, and those that contained more than three genes were used in this analysis. Details of this figure, including the genes and biological terms used, are provided in the Appendix 1 and Appendix 2. **C**: The relative expression of selected functional terms. The color represents the fold change in gene expression (cyan is used to represent those genes that are more expressed in MitoM, while purple is used for those genes more greatly expressed in RestM). Genes with a *t* test p value less than 0.01 and a fold change greater than 1 were used. The dashed lines mark twofold expression.

respectively. Conversely, CECs in the RestM condition showed higher expression levels of *FBLN5*, which is known to promote endothelial cell adhesion; *insulin-like growth factor (IGF)-1*, which promotes cell growth and development; and *TIMP3*, an inhibitor of matrix metalloproteinases (MMPs). These results suggested that CECs are involved in the remodeling in MitoM, while they are involved during assembly states in RestM. Other functional terms showed a similar number of genes that were more greatly expressed in either condition, such as those related to apoptosis, acetylation/phosphorylation, and response to stimulus. These terms require further analysis.

Validation of gene expression: To compare the results with native expression of transcripts and proteins from adult rabbits and to validate the microarray results, we performed qPCR and immunocytochemistry analyses of four genes. *ATP1A1*, *TJP1*, *GPC4*, and *BTG2* were selected for this purpose because they are good markers of CEC functions. We first tested the protein expression of TJP1 (ZO-1), an adult marker of CECs [20,21], which was also overexpressed in RestM, comparing the immunostaining in basal conditions from complete corneas with the growth in both conditions. The fluorescence images shown in Figure 4A support the previous results where the protein expression of ZO-1 was localized more clearly in membranes in cornea and RestM, whereas in MitoM the expression localization was diffuse. For ATP1A1, TJP1, and GPC4, the overall protein expression at P2 seems higher in RestM than in MitoM (Figure 4B), which is consistent with transcriptional measurements where three out of the four genes show a statistically significant increase in expression between RestM and MitoM (Figure 4C).

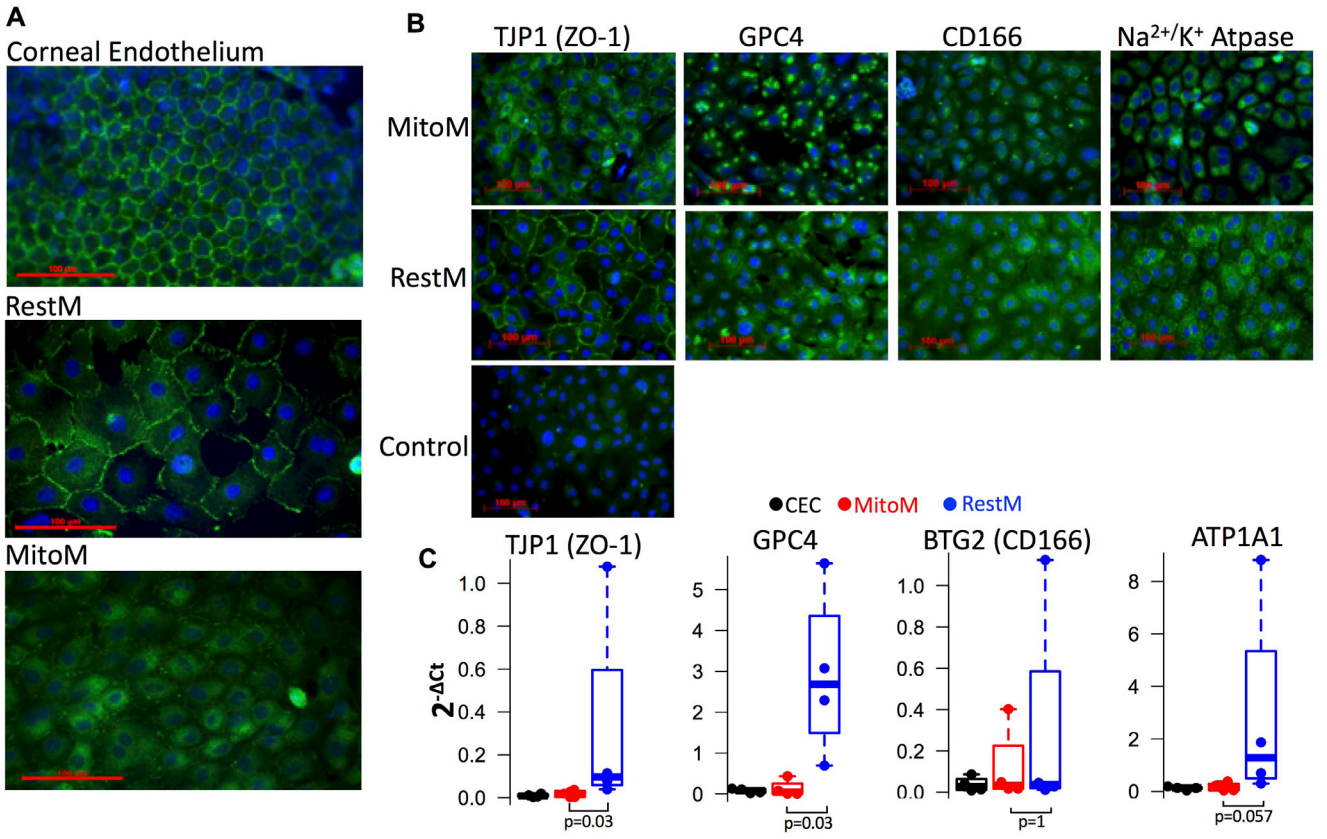

Figure 4. Comparison of protein and transcript expression. **A**: TJP1 / ZO-1 specific surface marker. 20X, immunostaining on flat-mounted cornea, corneal endothelium, basal condition respectively. **B**: 40X, immunocytochemistry of second passage cultured CECs upon a two-phase culture system. Specific surface markers were assessed upon a two-phase culture system. In RestM, tight junction zig-zag characteristic configuration is observed and well stablished between cells. In MitoM, weak fluorescent signal and lack of protein location. In control no primary antibody; exposure normalized for each antibody set. **C**: qPCR of markers in rabbit CECs (basal expression levels), MitoM condition or RestM condition. Ct values were normalized using GAPDH. ΔCT represent the difference in Ct values between GAPDH and the gene shown.

DISCUSSION

Culture methods for rabbit and human CEC culture have been previously reported. The culture of rabbit CECs using a supplemented medium demonstrated proliferation for up to 67 passages [22]. However, the CECs in the cited study exhibited chromosomal aneuploidy, and they presented a fibroblastic shape [22]. The changes made to a non-supplemented medium for 1 week (MEM 5% BCF) facilitated the recovery of the cells' polygonal shape. In human CECs, it was demonstrated that the combination of vascular endothelial growth factor (VEGF), EGF, fibroblast growth factor (FGF), and IGF yields better cell attachment and cuboidal morphology up to the first passage (approximately 10 days) when compared to the CECs in the basal media [8]. A different study reported that the use of a supplemented culture media, using the same composition of MitoM used in this study, resulted in polygonal CEC proliferation up until the fifth passage, but the expression of specific molecular markers was evident up until the second passage [6]. In a study in which four different media were used, the best outcomes in terms of proliferation, morphology, and molecular marker expression were obtained with the MitoM medium used here, as well as with another medium containing ascorbic acid, insulin–transferrin–sodium selenite (ITS), and bFGF. These two media allowed the CECs to retain their polygonal morphology, and they further expressed ZO-1 and Na/K-ATPase up until the third passage [10]. ZO-1 and Na/K-ATPase are markers of cell identity and the lack of epithelial to mesenchymal transition [23].

The same research group recently reported the use of a supplemented culture medium featuring ascorbic acid, ITS, and bFGF to proliferate CECs. This approach was coupled with a second step in which a maintenance medium (endothelial SFM 5% FBS) was used. In their method, human CECs were cultured for three passages, each consisting of 14 days in the supplemented medium and 7 days in the maintenance medium. This is different from our method, which involved culturing the cells for 5 days in MitoM until confluence, followed by two additional passages in RestM medium (where the composition was the same as in MitoM, but without growth factors). The authors of the previous work reported that the CECs demonstrated a spindle morphology when they were cultured in supplemented medium alone, and they exhibited an enhancement of cell circularity when the non-supplemented medium was added, which persisted throughout the three passages. In the present experiment, the CECs showed a spindle morphology when cultured in MitoM, and they recovered their polygonal morphology after 48 h in RestM, which persisted during the following passage in the same medium.

The results of these studies were in accordance with ours with respect to the recovery of the cells' polygonal morphology after the supplemented medium was changed to a basal medium. Further experiments will determine if multiple cycles of proliferation and recuperation retain the characteristics of CECs without demonstrating senescence. Meanwhile, we observed that shape was maintained around the fourth passage.

The role of cell senescence and culture media supplementation has been demonstrated in studies using human CECs. The protein tyrosine phosphate *PTP1B*, known to negatively regulate EGF-induced signaling by dephosphorylating the *EGF receptor* (*EGFR*), is more greatly expressed in CECs obtained from younger donors [14]. In this context, the proliferation response to an EGF stimulus in cultured CECs is dependent on the synergy between *PTP1B* and *EGFR*, and it is lower in older donor and senescent cells. This explains why the EGF stimuli response decreased in senescent cells even when the level of EGFR remained relatively constant. Our culture system prevented the CECs from entering into a senescent state by adding a stabilization step. The *PTP1B* gene was not among the differentially expressed genes observed for the CECs in MitoM and RestM, which could be an indicator of the potential of this system for corneal engineering.

To better understand the molecular mechanisms underlying the morphological changes recorded throughout the two-culture media, a microarray analysis was performed. The identification of the Gene Ontology (GO) term related to wound healing suggested that CECs in MitoM can act to signal tissue damage, and they further activate a series of events with the objective of restoring cell integrity following an injury. The movement of cells from the G1 to S phase implicates the inhibition of cell–cell contact [24]. Kimura demonstrated that in the presence of harmful stimuli, it is possible to redistribute tight junctions without affecting adherent junctions [25]. This result correlates with the present results, in which the biological process GO term cell adhesion molecule binding, the CC-GO adherens junction, and the pathway for the adherent junction were established, while no changes were observed for tight junctions. GO terms related to the actin cytoskeleton and the regulation of cell projection assembly suggest dynamic actin cytoskeletal organization. Actin cytoskeletal reorganization can be related to the protrusive forces involved in cell migration [26]. The identification of the MF-GO terms related to metalloendopeptidase activity, collagen metabolic processes, and collagen degradation, along with the GO-BP-positive regulation of catalytic activity, suggest that a catalytic

process is involved in extracellular collagen composition, which is controlled by MMPs. MMPs are important in the process of connective tissue remodeling [27], and they may be involved in the reorganization of the TJ protein seen in CECs in MitoM. CECs in MitoM did not express MMP inhibitors; thus, the changes in cell morphology could be related to dynamic actin cytoskeletal reorganization, changes in the extracellular matrix composition, and reorganization of the cell junctions.

CECs in RestM showed GO terms related to wound healing as well, such as focal adhesion, remodeling in the extracellular matrix, and extracellular matrix receptor interaction, which suggests that RestM also acts as a signal to indicate damage, ultimately activating a series of events related to restoring the monolayer's integrity. The polygonal morphology seen in CECs in RestM is a good index of the progress of endothelial restoration [28], and together with the rearrangement of the cytoskeleton, it recalls the tissue remodeling state. The expression of collagen IV suggests that RestM can promote the reestablishment of the structure and composition of the extracellular matrix, which is essential for the attachment of CECs to DM. qPCR validated the difference in the expression of the *ATP1A1, TJP1,* and *GPC4* genes among the CECs before culture, in MitoM, and in RestM. The CECs in RestM showed higher expression level of these markers. However, the expression levels were higher than those observed in basal CECs. We hypothesize that activation of the proliferative state during MitoM before the RestM condition could lead to these results. Because we analyzed the expression level at 80% cell confluence, expression levels during an increased rate of transcription were obtained, in contrast to basal expression, in which corneal endothelium is in an expression steady-state. Further experiments with a different rate of confluence would confirm these insights. Immunocytochemistry analysis demonstrated similar locations and expression levels of TJP1/ZO-1 in flat CE and in CECs in RestM. In addition, CECs in RestM showed higher expression of adult CE markers GPC4 and Na/K-ATPase compared to CECs in MitoM.

The differentially expressed genes obtained in this system are similar to those reported by Peh et al. following the use of a different proliferative medium coupled with a maintenance medium [29]. Cell proliferation and wound healing were among the top pathways evident in both approaches. Although there are methodological differences between their study and the present study, the results demonstrated the effectiveness of a coupled system in the proliferation of CECs, as well as in the maintenance of their morphological and molecular characteristics. Further in vivo analyses will determine the efficacy of CECs cultured with these systems in restoring corneal function.

It has been shown that the proliferative capacity of CECs is age-dependent in humans and rabbits [30,31]. In the present experiments, we used 3-month-old rabbits which show high mitotic activity. It would be interesting to compare the behavior of the present culture system at different ages.

CONCLUSIONS: We showed a two-phase system with novel medium and transcriptome data, analysis, and validation. Other research groups used a different medium [29] or did not analyze the transcriptome [32]. The differences in the morphology, pathways, and gene expression observed between CECs in RestM and MitoM suggest that although MitoM enhances CEC proliferation, it could result in cell differentiation and drive the culture to exhibit a wound-like state. The resting step facilitated the recovery of the cells' hexagonal shape; it further benefitted the maintenance of pump function, cell-cycle arrest, the cells' barrier function (via junction reorganization), the reconstruction of the extracellular matrix's structural constituent, and the production of collagen IV (a component of DM), all of which are related to the final events involved in remodeling during the wound-healing process.

Future experiments focused on analyzing the number of cycles in which the CECs cultured in this system are able to proliferate and recover specific markers will provide additional evidence for this system's potential in regenerative medicine. Cells cultured in this system may ultimately address the shortage of tissue donors available for corneal grafts.

APPENDIX 1. CECS ISOLATION USING ENZYMATIC DIGESTION.

To access the data, click or select the words "Appendix 1." A) Tissue conglomerates obtained after collagenase I treatment. B) Cell clusters obtained after trypsin/EDTA treatment. C) Adherent cells after enzymatic digestion.

APPENDIX 2. FUNCTIONAL ANALYSIS OF DIFFERENTIALLY EXPRESSED GENES.

To access the data, click or select the words "Appendix 2." The heat map shows the genes (horizontal axis) contained within functional biologic terms (vertical axis). The color represents the fold change in gene expression (cyan is used to represent those genes that were more greatly expressed in MitoM, while purple represents those genes more greatly expressed in RestM). Genes whose *t* test p values were <0.01, and which demonstrated a fold change >1, were used. Only

over-represented biologic terms with a p value <0.01, a false discovery rate <0.25, and those that contained >3 genes were used in this analysis.

ACKNOWLEDGMENTS

English-language editing of this manuscript was provided by Journal Prep. This work was funded by Consejo Nacional de Ciencia y Tecnología (CONACyT) grant PN6558 and Tecnologico de Monterrey.

REFERENCES

1. Bonanno JA. Identity and regulation of ion transport mechanisms in the corneal endothelium. Prog Retin Eye Res 2003; 22:69-94. [PMID: 12597924].
2. Schmedt T, Silva MM, Ziaei A, Jurkunas U. Molecular bases of corneal endothelial dystrophies. Exp Eye Res 2012; 95:24-34. [PMID: 21855542].
3. Oliva MS, Schottman T, Gulati M. Turning the tide of corneal blindness. Indian J Ophthalmol 2012; 60:423-7. [PMID: 22944753].
4. Lass JH, Gal RL, Dontchev M, Beck RW, Kollman C, Dunn SP, Heck E, Holland EJ, Mannis MJ, Montoya MM, Schultze RL, Stulting RD, Sugar A, Sugar J, Tennant B, Verdier DD. Donor age and corneal endothelial cell loss 5 years after successful corneal transplantation. Specular microscopy ancillary study results. Ophthalmology 2008; 115:627-32. e8. [PMID: 18387408].
5. Joyce NC. Cell cycle status in human corneal endothelium. Exp Eye Res 2005; 81:629-38. [PMID: 16054624].
6. Vianna LM, Kallay L, Toyono T, Belfort R Jr, Holiman JD, Jun AS. Use of human serum for human corneal endothelial cell culture. Br J Ophthalmol 2015; 99:267-71. .
7. Nakahara M, Okumura N, Kay EP, Hagiya M, Imagawa K, Hosoda Y, Kinoshita S, Koizumi N. Corneal endothelial expansion promoted by human bone marrow mesenchymal stem cell-derived conditioned medium. PLoS One 2013; 8:e69009-[PMID: 23894393].
8. Choi JS, Kim EY, Kim MJ, Khan FA, Giegengack M, D'Agostino R Jr, Criswell T, Khang G, Soker S. Factors affecting successful isolation of human corneal endothelial cells for clinical use. Cell Transplant 2014; 23:845-54. [PMID: 23461892].
9. Zhu C, Joyce NC. Proliferative response of corneal endothelial cells from young and older donors. Invest Ophthalmol Vis Sci 2004; 45:1743-51. [PMID: 15161835].
10. Peh GS, Toh KP, Wu FY, Tan DT, Mehta JS. Cultivation of human corneal endothelial cells isolated from paired donor corneas. PLoS One 2011; 6:e28310-[PMID: 22194824].
11. Joyce NC. Proliferative capacity of corneal endothelial cells. Exp Eye Res. 95. England: 2011 Elsevier Ltd; 2012. p. 16–23.
12. Kim E, Kim JJ, Hyon JY, Chung ES, Chung TY, Yi K, Wee WR, Shin YJ. The effects of different culture media on human corneal endothelial cells. Invest Ophthalmol Vis Sci. 55. United States: 2014 The Association for Research in Vision and Ophthalmology, Inc.; 2014. p. 5099–108.
13. Noh JW, Kim JJ, Hyon JY, Chung ES, Chung TY, Yi K, Wee WR, Shin YJ. Stemness Characteristics of Human Corneal Endothelial Cells Cultured in Various Media. Eye Contact Lens 2015; 41:190-6. [PMID: 25603434].
14. Ishino Y, Zhu C, Harris DL, Joyce NC. Protein tyrosine phosphatase-1B (PTP1B) helps regulate EGF-induced stimulation of S-phase entry in human corneal endothelial cells. Mol Vis 2008; 14:61-70. [PMID: 18253097].
15. Schneider CA, Rasband WS, Eliceiri KW. NIH Image to ImageJ: 25 years of image analysis. Nat Methods 2012; 9:671-[PMID: 22930834].
16. Laboratories HAI. Inc. Visual Atlas of Eye Bank Specular Microscopy – Donor Corneal Endothelium Imaging. 2013: 2–3. Available from: http://hailabs.com/wp-content/uploads/2014/05/Visual-Atlas-of-Eye-Bank-Specular-Microscopy.pdf
17. Peh GSL, Toh K-P, Ang H-P, Seah X-Y, George BL, Mehta JS. Optimization of human corneal endothelial cell culture: density dependency of successful cultures in vitro. BMC Res Notes 2013; 6:176-[PMID: 23641909].
18. Dennis G Jr, Sherman BT, Hosack DA, Yang J, Gao W, Lane HC, Lempicki RA. DAVID: Database for Annotation, Visualization, and Integrated Discovery. Genome Biol 2003; 4:3-[PMID: 12734009].
19. Forest F, Thuret G, Gain P, Dumollard J-M, Peoc'h M, Perrache C, Zhiguo H. Optimization of immunostaining on flat-mounted human corneas. Mol Vis 2015; 21:1345-56. [PMID: 26788027].
20. Yoshihara M, Ohmiya H, Hara S, Kawasaki S, Hayashizaki Y, Itoh M, Kawaji H, Tsujikawa M, Nishida K. Discovery of molecular markers to discriminate corneal endothelial cells in the human body. PLoS One 2015; 10:e0117581-[PMID: 25807145].
21. Zavala J, Lopez Jaime GR, Rodriguez Barrientos CA, Valdez-Garcia J. Corneal endothelium: developmental strategies for regeneration. Eye (Lond) 2013; 27:579-88. [PMID: 23470788].
22. Fan T, Zhao J, Fu Y, Cong R, Guo R, Liu W, Han B, Yu Q, Wang J. Establishment of a novel corneal endothelial cell line from domestic rabbit, Oryctolagus curiculus. Sci China C Life Sci 2007; 50:161-9. [PMID: 17447022].
23. Kinoshita S, Koizumi N, Ueno M, Okumura N, Imai K, Tanaka H, Yamamoto Y, Nakamura T, Inatomi T, Bush J, Munetoyo T, Michio H. Injection of Cultured Cells with a ROCK Inhibitor for Bullous Keratopathy. N Engl J Med 2018; 378:995-1003. [PMID: 29539291].
24. Senoo T, Obara Y, Joyce NC. EDTA: a promoter of proliferation in human corneal endothelium. Invest Ophthalmol Vis Sci 2000; 41:2930-5. [PMID: 10967047].

25. Kimura K, Teranishi S, Nishida T. Interleukin-1beta-induced disruption of barrier function in cultured human corneal epithelial cells. Invest Ophthalmol Vis Sci 2009; 50:597-603. [PMID: 19171646].

26. Tondeleir D, Lambrechts A, Muller M, Jonckheere V, Doll T, Vandamme D, Bakkali K, Waterschoot D, Lemaistre M, Debeir O, Decaestecker C, Hinz B, Staes A, Timmerman E, Colaert N, Gevaert K, Vandekerckhove J, Ampe C. Cells lacking beta-actin are genetically reprogrammed and maintain conditional migratory capacity. Mol Cell Proteomics 2012; 11:255-71. [PMID: 22448045].

27. Shimoda M, Ishizaki M, Saiga T, Yamanaka N. Expression of matrix metalloproteinases and tissue inhibitor of metalloproteinase by myofibroblasts–morphological study on corneal wound healing. Nippon Ganka Gakkai Zasshi 1997; 101:371-9. [PMID: 9170840].

28. Krachmer JH, Mannis MJ, Holland E, Cornea J. Fundamentals, Diagnosis and Management. Volume 1. 2nd Ed. Elsevier Mosby, Philadelphia USA, 2005

29. Peh GS, Chng Z, Ang HP, Cheng TY, Adnan K, Seah XY, George BL, Toh KP. Tan Dt, Ym GH, Colman A, Mehta JS. Propagation of human corneal endothelial cells: a novel dual media approach. Cell Transplant 2015; 24:287-304. [PMID: 24268186].

30. Contreras-Corona RG, Anaya-Pava EJ, Gallegos-Valencia AJ, Villarreal-Maíz JA. Densidad y morfología de células del endotelio corneal en adultos jóvenes del norte de México. Revista Mexicana de Oftalmología. 2014; 88:99-103. .

31. Valdez-Garcia JE, Lozano-Ramirez JF, Zavala J. Adult white New Zealand rabbit as suitable model for corneal endothelial engineering. BMC Res Notes 2015; 82015:28-[PMID: 25648773].

32. Bartakova A, Kuzmenko O, Alvarez-Delfin K, Kunzevitzky NJ, Goldberg JL. A Cell Culture Approach to Optimized Human Corneal Endothelial Cell Function. Invest Ophthalmol Vis Sci 2018; 59:1617-29. [PMID: 29625488].

Articles are provided courtesy of Emory University and the Zhongshan Ophthalmic Center, Sun Yat-sen University, P.R. China. The print version of this article was created on 14 November 2019. This reflects all typographical corrections and errata to the article through that date. Details of any changes may be found in the online version of the article.